BMC Cancer

RESEARCH Open Access

Radiomics feature is a risk factor for locally advanced cervical cancer treated using concurrent chemoradiotherapy based on magnetic resonance imaging: a retrospective study

Yuan Wang[1], Yanyan Yu[2], Lina Gu[1], Yunfeng Sun[2], Jiazhuo Yan[1], Hongxia Zhang[2] and Yunyan Zhang[1*]

Abstract

Background Although concurrent chemoradiotherapy (CCRT) is the standard treatment strategy for locally advanced cervical squamous carcinoma (LACSC), there are still individual differences. It is of vital importance to establish a radiomics-based model for predicting overall survival (OS) of LACSC patients treated using CCRT, and evaluating the feasibility of adjuvant chemotherapy (ACT).

Methods 122 LACSC patients were retrospectively analyzed who underwent pelvic MRI before standard CCRT between January 2013 and September 2016, including 85 patients in training set and 37 patients in testing set. 3D Slicer was used to segment images and extract features. IPMs software was used to select features and construct radscore. We selected the group with the largest area under the curves as the best result from 150 feature subsets and corresponding radscore. A nomogram was established using univariate and multivariate Cox analyses. We used Shapley Additive Explanations (SHAP) for further interpretation of the nomogram. Kaplan–Meier curves demonstrated the associations of radscore and clinical characteristics with OS and ACT.

Results Radscore was a prognostic factor ($P=0.001$) which constructed using 10 radiomics features influencing the OS of patients with LACSC treated using CCRT. The radiomics-clinical model estimated OS (training, C-index: 0.761; testing, C-index: 0.718) more accurately than the clinical (training, C-index: 0.745; testing, C-index: 0.708) and radiomics models (training, C-index: 0.702; testing, C-index: 0.671). Radscore has the greatest impact on the prognosis of LACSC patients. We combined radscore and clinical factors to obtain risk scores. There was a better OS rate among low-risk patients than among high-risk patients (training, $P=0.034$; testing, $P=0.003$). Compared with CCRT, ACT + CCRT did not improve prognosis (high-risk patients, $P=0.703$; all patients, $P=0.425$).

Conclusions Radscore independently predicted OS in LACSC. The radiomics-clinical nomogram improved individualized OS estimation. Patients did not benefit from ACT.

*Correspondence:
Yunyan Zhang
zhangyunyan@hrbmu.edu.cn

Full list of author information is available at the end of the article

Keywords Cervical cancer, Radiomics, Magnetic resonance imaging, Overall survival, Concurrent chemoradiotherapy

Introduction

Cervical cancer is a common gynecological malignant tumor, which seriously threatens women's health. The disease is locally advanced in 35% of cervical cancer patients when they are diagnosed [1]. Concurrent radiotherapy combined with platinum-based chemotherapy is the standard treatment for locally advanced cervical squamous carcinoma (LACSC). However, there is a high risk of local recurrence and distant metastasis, and the 5-year overall survival (OS) rate is only 17.6% [2]. To improve the survival of LACSC patients, clinicians have attempted multiple strategies, including increased radiation dose, adjuvant chemotherapy (ACT), and targeted therapy [3]. However, there are still differences in the efficacy of the same treatment regimen for different patients, and the addition of adjuvant therapy also poses additional adverse side effects and economical burdens for patients and their families. Therefore, it is urgent for clinicians to determine a biomarker that can predict the efficacy of concurrent chemoradiotherapy (CCRT) in patients with LACSC.

The therapeutic effect of ACT after CCRT for LACSC is controversial. Duenas-Gonzalez et al. [4] reported that ACT could reduce the risk of distant metastasis. Another study reported that ACT significantly improved the 3-year distant metastasis-free survival rate of patients with stage IIIC1r cervical cancer [5]. Choi et al. [6] confirmed the efficacy of ACT, but noted that its toxicity and side effects were severe. The feasibility of ACT after CCRT is uncertain, and this treatment is not suitable for all cervical cancer patients [7–9]. Therefore, identifying patients who require ACT after CCRT is challenging and necessary.

Radiomics is a novel scientific field in which large amounts of high-dimensional quantitative features are extracted from medical images, and then correlations between these features are mined to aid in determining diagnosis or prognosis [10]. Compared with conventional radiography in which analysis is usually performed by visual inspection, radiomics introduces an innovative way to mine medical images for more detailed information, and is expected to provide valuable information for accurate treatment and prognosis assessment [11]. Thus far, we could use radiomics to predict the conditions of cervical cancer patients, such as tumor stage, histological tumor type, tumor recurrence, and OS [12]. However, few studies have applied radiomics to predict the survival of LACSC patients after CCRT. Thus, we aimed to develop a new prognostic model for cervical cancer after CCRT by combining radiomics features and clinical characteristics. Furthermore, we aimed to use this model to determine whether ACT is beneficial in patients with LACSC after CCRT.

Methods

Patients and clinical characteristics

In this study, there were 122 patients diagnosed with LACSC and treated using CCRT at Harbin Medical University Cancer Hospital Department of Gynecological Radiotherapy from January 2013 to September 2016 (Fig. 1). The inclusion criteria were as follows: (1) LACSC as confirmed by cervical biopsy (International Federation of Gynecology and Obstetrics [FIGO] 2018 stages IB3–IVB), (2) magnetic resonance imaging (MRI) within 14 days before treatment (including at least pelvic T2-weighted imaging [T2WI]), (3) treated using CCRT, (4) no history of radiotherapy or chemotherapy, and (5) available clinicopathological data. The exclusion criteria were as follows: (1) unsatisfactory MRI scans (image loss, poor quality, or no pelvic T2WI), (2) non-standard treatment (total dose of external radiotherapy < 45 Gy or no cisplatin-containing CCRT), and (3) incomplete case information. We collected clinical characteristics from patients' medical records, including age, SCC antigen level, FIGO stage and tumor size, and re-evaluated all patients using FIGO 2018 stages.

Treatment and follow-up

All patients received CCRT consisting of pelvic external radiation therapy, concurrent platinum-containing chemotherapy, and brachytherapy. Five times a week, 1.8 Gy were delivered for a total of 45–50 Gy performed with Intensity-modulated radiation therapy (IMRT). Metastatic lymph nodes in stage IIIC1 patients were treated with radical dose radiotherapy with Simultaneously Integrated Boosted (SIB). Combined with brachytherapy, the local dose of cervix could also reach the radical dose. A weekly dose of cisplatin (40 mg/m^2) was administration intravenously with radiotherapy (day 1). An intravitreal brachytherapy protocol was used with 4–6 fractional delivering 6–7 Gy and a total 30–36 Gy at point A. For patients with SCC ≥ 10ng/mL and FIGO 2018 staging beyond stage IIIB, ACT with paclitaxel plus cisplatin or paclitaxel plus carboplatin was given 21 days after the end of CCRT for 1 cycle every 21 days for 2 to 3 cycles. The treatment plan was adjusted according to the patient's health status and blood indicators. The endpoint of OS was defined as the period of time between the start of treatment and death from any cause. The hospital follow-up center followed up the patients every month, every three months and every six months, and told the

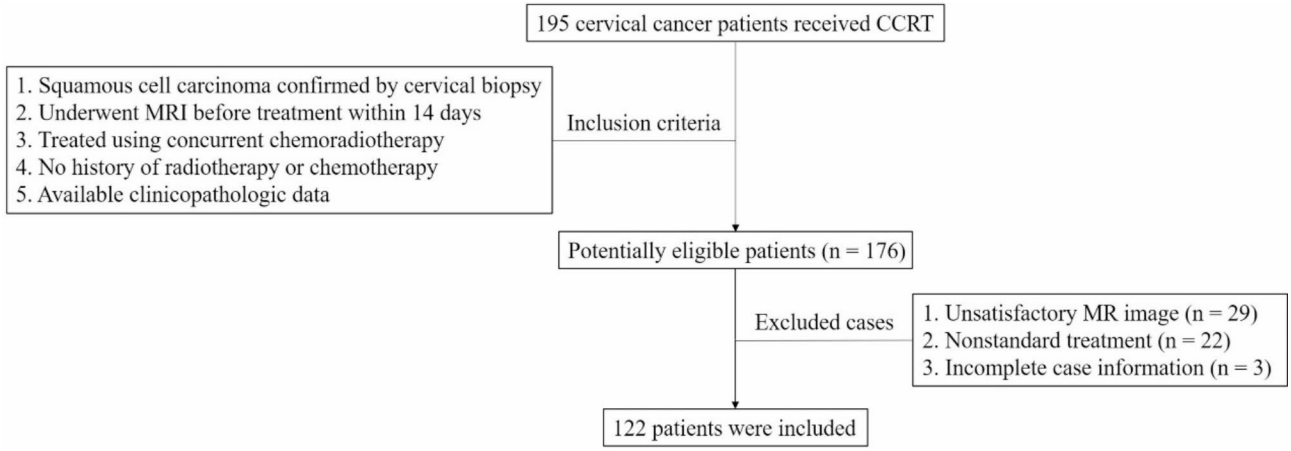

Fig. 1 Flow chart of patient recruitment

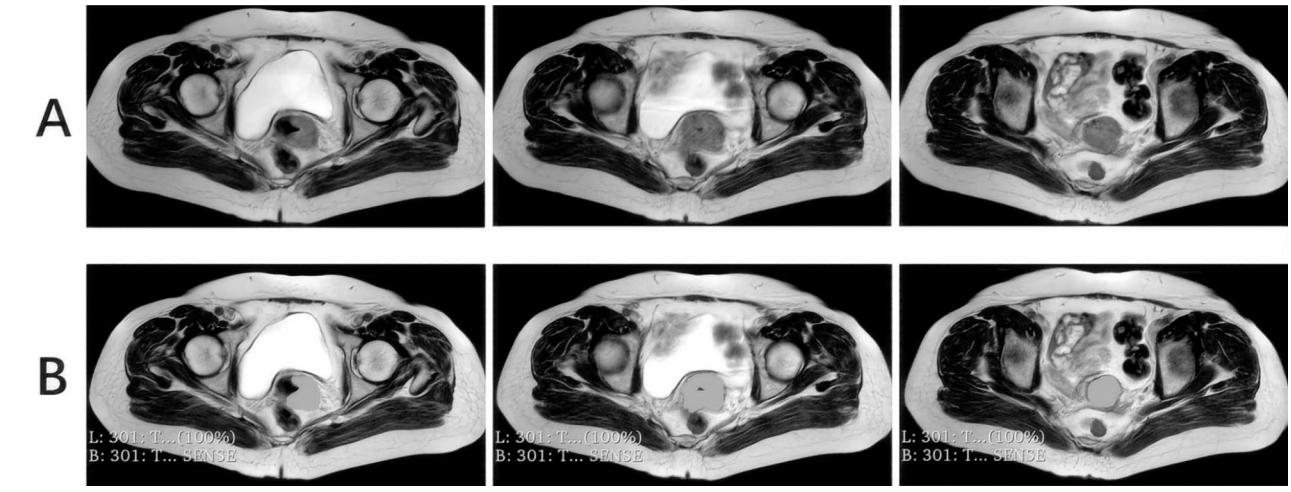

Fig. 2 Tumor segmentation on every slice showing the tumor. (**A**) Raw images. (**B**) Corresponding tumor segmentation

patients to review regularly. Patients were monitored until September 2021.

MRI protocol

In all cases, routine pelvic MRI was administered within 14 days before the treatment. Axial pelvis MRI was performed using a clinical whole-body scanner (Philips Ingenia 3.0T) and a phased-array 16-channel sensitivity encoding abdominal coil. The scanning parameters were as follows: repetition time, 2700 ms; echo time, 90 ms; field of view, 280 × 431 mm; matrix, 340 × 374; 32 slices; and slice thickness, 6 mm. In a supine position, patients were introduced to maintain stable breathing to reduce respiratory interference. An entire pelvis was covered by the scan. Because of the differences in scan protocol, we only selected relatively consistent T2WI for the study.

Radiomics analysis: image segmentation

A radiologist (YYY, with 5-year experience) used 3D Slicer (version 4.11.20200930, https://www.slicer.org) for the manual segmentation of axial T2WI that covered the total tumor area, while avoiding areas of necrosis or hemorrhage, and adjacent vessels as much as possible (Fig. 2). And subsequently the segmentation was reviewed by a radiologist (HXZ) with > 20-year experience.

Radiomics analysis: feature extraction

Radiomics features were automatically calculated by 3D Slicer (version 4.11.20200930). Totally, 851 radiomics features were extracted from axial MRI scans, including (1) shape features, such as major axis length, sphericity and voxel volume; (2) first-order features, such as energy, interquartile range, mean absolute deviation, range, and root mean squared; and (3) texture features, such as gray-level co-occurrence matrix (GLCM), neighborhood gray-tone difference matrix, and gray-level dependence matrix (GLDM).

Radiomics analysis: feature selection

We used univariate and multivariate Cox proportional risk models to select features associated with survival by IPMs software (version 2.4.3). IPMs is a software developed to simplify the statistical analysis progress, which was developed by Precision Health Institution of GE Healthcare. Cox proportional risk model was univariately significant at 0.05. We randomly divided patients into training set and testing sets. In the training dataset, optimal feature subsets were used to develop a Cox-based radscore model. In total, we obtained 150 feature subsets and their corresponding radscores. After plotting the receiver operating characteristic (ROC) curve on survival, the group with the largest area under the curve (AUC) was chosen as the best result.

Prognostic model construction

The cutoff values of factors were determined by ROC curves based on the Youden index, and Kaplan–Meier curves generated for OS. Kaplan–Meier curves were compared using the log-rank test. Significant clinical variables were identified using univariate and multivariate Cox regression models ($P < 0.05$). We developed a nomogram to predict an individual's OS in order to facilitate clinical use.

Statistics

All statistical analyses of radiomics data in the present study were performed using R software (version 3.5.1) and Python software (version 3.11). RStudio (version 4.1.2) was used for model construction, C-index calculation, and calibration curve plotting. C-indices and 95% confidence intervals (CIs) were used to quantify and compare the discrimination between each model. Predicted and observed probabilities were evaluated using calibration curves. We used R packages, including rms, survival, and Hmisc, in this study. Pycharm-community-2023.3.4 was used for Shapley Additive Explanations (SHAP). Cutoff values of radscore, SCC antigen level, FIGO stage and tumor size were determined using Medcalc software (version 11.4.2.0). The probabilities of OS was estimated by the Kaplan-Meier method and compared using log-rank test. IBM SPSS software (version 25) was used to perform all survival analyses and COX regression analyses, and Graphpad Prism10 software was used for plotting. It was statistically significant when the *P* value was less than 0.05.

Table 1 Patient characteristics

Characteristic	Training set ($n=85$)	Testing set ($n=37$)	*P* value
Age (years)	56.4 ± 8.5	60 ± 10.5	0.206
FIGO stage (2018)			0.570
IB	3 (3.5%)	0 (0%)	
IIA	0 (0%)	1 (2.7%)	
IIB	33 (38.8%)	12 (32.4%)	
IIIA	4 (4.7%)	2 (5.4%)	
IIIB	33 (38.8%)	16 (43.2%)	
IIIC1	10 (11.8%)	4 (10.8%)	
IVB	2 (2.4%)	2 (5.4%)	
Tumor size			0.657
≤30 mm	17 (20%)	8 (21.6%)	
>30 mm	68 (80%)	29 (78.4%)	
SCC antigen			0.549
≤4.7 ng/mL	33 (38.8%)	17 (45.9%)	
>4.7 ng/mL	52 (61.2%)	20 (54.1%)	
Adjuvant chemotherapy			0.263
Yes	66 (77.6%)	25 (67.6%)	
No	19 (22.4%)	12 (32.4%)	
P value	0.196	0.243	

FIGO, International Federation of Gynecology and Obstetrics; SCC, squamous cell carcinoma

Results

General characteristics of training and testing sets

As shown in Table 1, the 122 enrolled patients had the following characteristics. All patients had an ECOG performance status 0 or 1. The patients were randomly classified into a training set ($n=85$) and a testing set ($n=37$) using IPMs software. There were no significant differences between the training and testing sets. And there were no significant differences between patients with and without ACT in both training and testing sets.

Constructing radiomics signatures based on feature selection

A total of 10 radiomics features were considered as factors influencing the survival of patients with LACSC treated using CCRT: major axis length, large area high gray level emphasis, run length nonuniformity normalized, informational measure of correlation, Matthews correlation coefficient, zone variance, cluster shade, dependence variance, large dependence low gray level emphasis and large area low gray level emphasis.

Using the above features, we constructed a radscore model. The median radscore was −0.0586, and ROC curve analysis showed that the best cutoff threshold of the radscore was −0.3557 (AUC = 0.677). Using this optimum threshold, patients were divided into low- radscore (≤ -0.3557) and high- radscore (> -0.3557) groups. We found that in the training set, radscore was significantly associated with OS ($P=0.010$), and this result was confirmed in the testing set ($P=0.010$) according to the Kaplan–Meier survival curves (Fig. 3).

Clinical characteristic selection

ROC curves showed that the best cutoff threshold of squamous cell carcinoma (SCC) antigen was 4.7 ng/mL (AUC = 0.748). According to the Kaplan–Meier curves

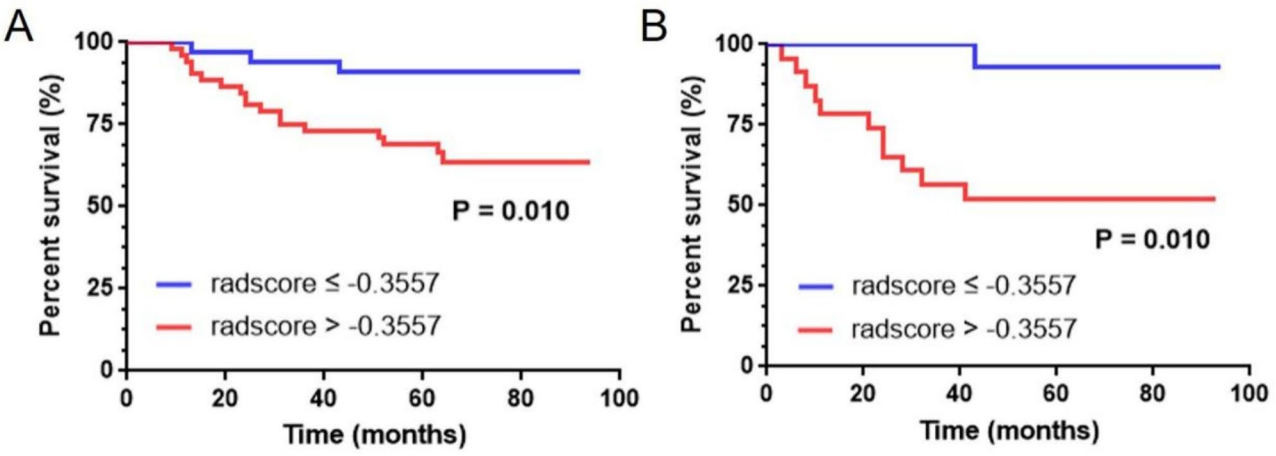

Fig. 3 Kaplan–Meier survival curves of radiomics signature. Stratified according to radscore, for patients in the training set (**A**) and testing set (**B**). Blue represents patients with radscore ≤ -0.3557, and red represents patients with radscore > -0.3557

(Fig. 4A, B), both training set and testing set showed significant association between SCC antigen level and OS ($P = 0.007$, $P = 0.016$, respectively). Figure 4C, D showed the Kaplan–Meier survival curves for the FIGO stage in the training set and testing set. The *P* values were 0.009 and 0.193, respectively. For tumor size, ROC curve analysis showed that the best cutoff threshold was 30 mm (AUC = 0.585). Based on the Kaplan–Meier curves estimation of the testing set, a significant difference in OS was found between two groups ($P = 0.041$; Fig. 4E). In the training set, smaller tumors (≤ 30 mm) exhibited better survival than larger tumors (> 30 mm), but there was no statistically significant difference ($P = 0.189$; Fig. 4F). FIGO stage ($P = 0.052$) and SCC antigen level ($P = 0.004$) independently predicted OS in a multivariate Cox analysis (Table 2).

Performance and validation of predictive models

According to the above results, we developed three prediction models: a radiomics model, a clinical model, and a combined model. Training and testing sets of the clinical model had C-indices of 0.745 (95% CI: 0.645–0.845) and 0.708 (95% CI: 0.573– 0.843), respectively. According to the training and testing data, the C-indices were 0.702 (95% CI: 0.584–0.821) and 0.671 (95% CI: 0.536–0.806) for the radiomics model. Using the clinical and radiomics model together, we achieved a C-index of 0.761 (95% CI: 0.655–0.867) in the training set and 0.718 (95% CI: 0.579–0.857) in the testing set (Table 3). Based on the clinical characteristics and radscore, a nomogram could be developed to predict the OS probability individually (Fig. 5A, B). Calibration curves indicated that predicted OS and actual OS were highly correlated (Fig. 5C, D).

SHAP

SHAP can explain the output of any machine learning model. Therefore, we used SHAP to increase the interpretability of the clinical-radiomics model in this study. Figure 6A is SHAP feature summary plots are summary plots of the influence of features on combined model and interactions between clinical characteristics and radiomics features. A positive SHAP value indicates an increased risk of predicting poor prognosis and vice versa. The higher the value, the higher the risk of poor prognosis. Each point corresponds to one predicted value for the participant. Figure 6B is SHAP bar chart which shows how each feature contributes to the overall prediction result, and the length of the bar represents the contribution size. We could find radscore plays the most important role in predicting OS of LACSC patients.

Kaplan–Meier survival analysis

We combined the FIGO stage, SCC antigen level, and radscore to obtain a novel risk score. ROC curves showed that the best cutoff threshold of the novel risk score was 0.5095 (AUC = 0.733). As a result of stratifying patients into low-risk and high-risk groups, the high-risk patients had significantly shorter OS, in comparison with the low-risk patients (training set: $P = 0.034$; testing set: $P = 0.003$; Fig. 5E, F).

Adjuvant chemotherapy

We divided patients into two groups according to whether they received ACT after CCRT. No significant differences in OS were found between those receiving CCRT alone and those receiving CCRT plus ACT in either high-risk cohort ($P = 0.703$; Fig. 7A) or overall study cohort ($P = 0.425$; Fig. 7B).

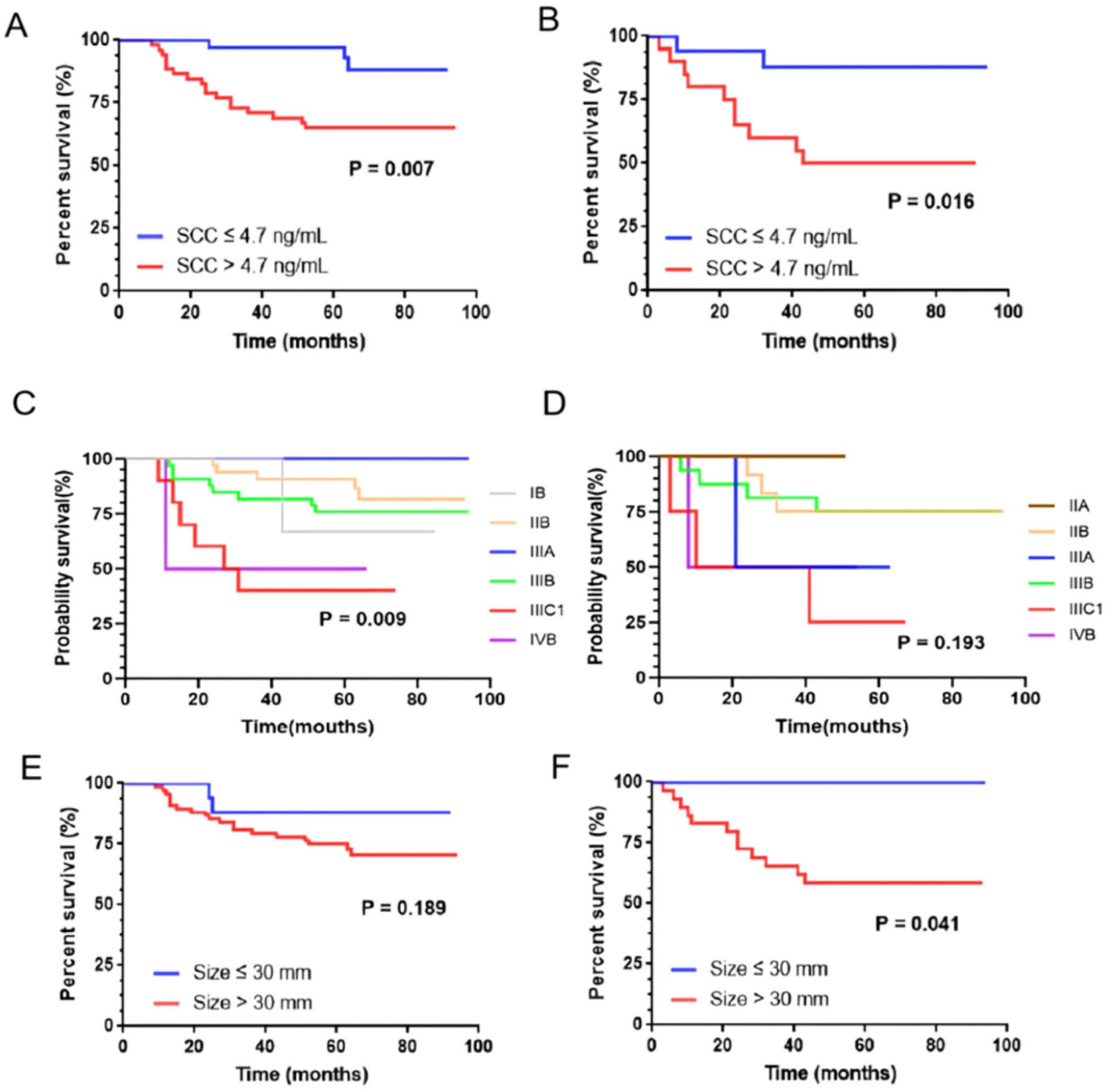

Fig. 4 Kaplan–Meier survival curves of clinical characteristics. Stratified according to SCC antigen levels, for patients in the training set (**A**) and testing set (**B**). Blue represents patients with SCC ≤ 4.7 ng/mL, and red represents patients with SCC > 4.7 ng/mL. Stratified according to FIGO stage, for patients in the training set (**C**) and testing set (**D**). The *P* values represent the correlation between the FIGO stage and overall survival. Gray represents patients with stage IB, brown represents patients with stage IIA, orange represents patients with stage IIB, blue represents patients with IIIA, green represents patients with stage IIIB, red represents patients with IIIC1, and purple represents patients with IVB. Stratified according to tumor size, for patients in the training set (**E**) and testing set (**F**). Blue represents patients with tumor size ≤ 30 mm, and red represents patients with tumor size > 30 mm. SCC, squamous cell carcinoma; FIGO, International Federation of Gynecology and Obstetrics

Table 2 Multivariate analysis of overall survival

Characteristic	B	Odds ratio	95% CI	*P* value
FIGO stage (2018)	0.259	1.295	0.997–1.682	0.052
SCC antigen level	1.520	4.573	1.622–12.892	0.004
Tumor size	-0.106	0.899	0.404–1.999	0.794

CI, confidence interval; FIGO, International Federation of Gynecology and Obstetrics; SCC, squamous cell carcinoma

Table 3 Performance of three prediction models

Model	Training set		Testing set	
	C-index	95% CI	C-index	95% CI
Radiomics model	0.702	0.584–0.821	0.671	0.536–0.806
Clinical model	0.745	0.645–0.845	0.708	0.573–0.843
Combined model	0.761	0.655–0.867	0.718	0.579–0.857

CI, confidence interval

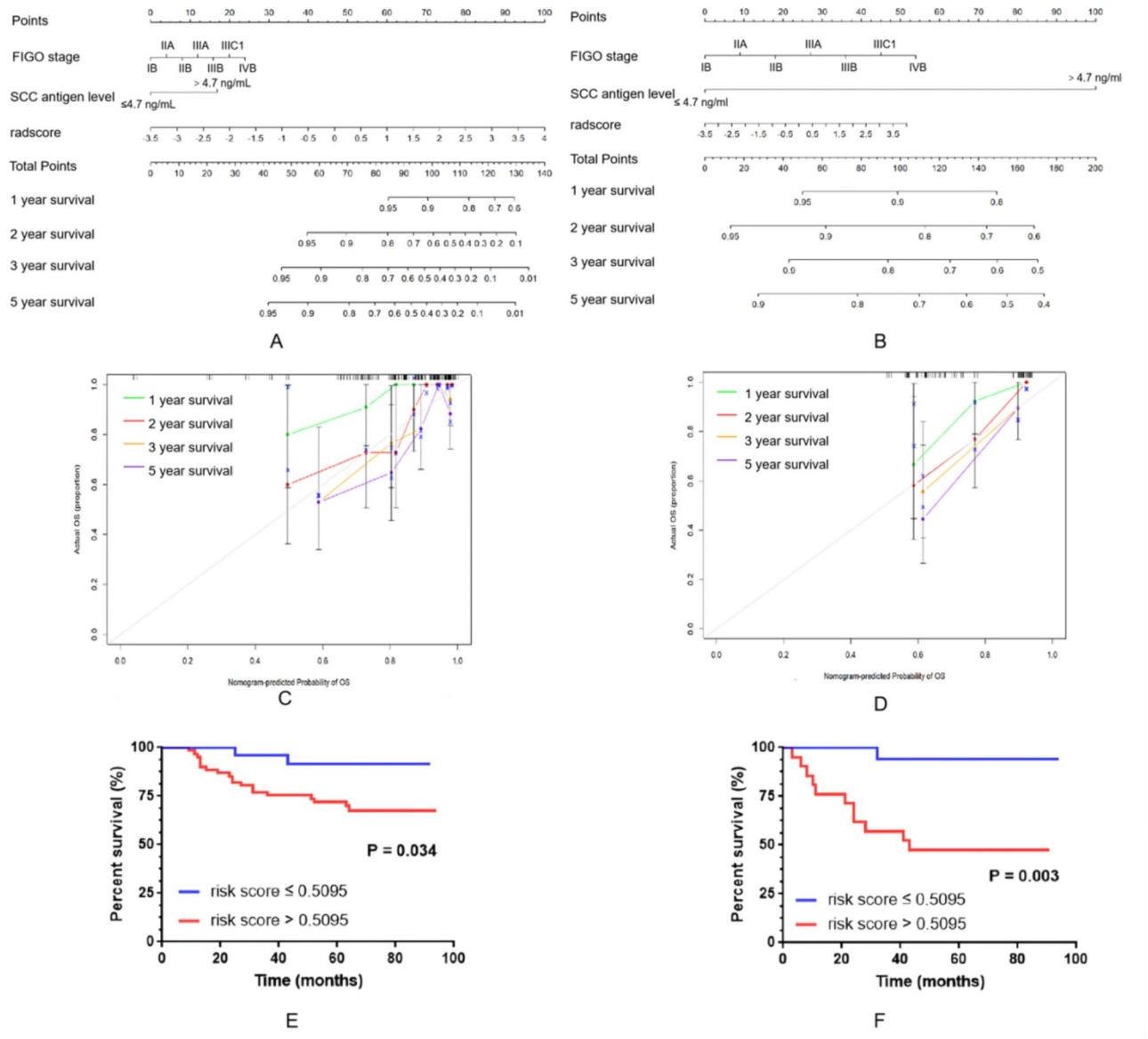

Fig. 5 Radiomics-clinical model and corresponding novel risk score. Nomograms based on clinical characteristics and radscore were used to estimate overall survival in the training set (**A**) and testing set (**B**). Calibration curves for the nomogram in the training set (**C**) and testing set (**D**). Green represents 1 year survival, red represents 2 year survival, orange represents 3 year survival, and purple represents 5 year survival. Kaplan–Meier survival curves, stratified according to the novel risk score, for patients in the training set (**E**) and testing set (**F**). Blue represents patients with risk score ≤ 0.5095, and red represents patients with risk score > 0.5095 mm. FIGO, International Federation of Gynecology and Obstetrics; SCC, squamous cell carcinoma; OS, overall survival

Discussion

In this study, we explored and validated a radiomics signature based on MRI data as a new biomarker to predict the prognosis of LACSC patients undergoing CCRT. We could only evaluate cervical cancer through the naked-eye observation of MRI scans, but radiomics signatures could provide more information about the tumor. The combination of the radiomics signatures and clinical characteristics was more accurate for the assessment of the patients' prognosis, and we also emphasized the importance of radiomic features. In accordance with the combined model, 122 patients were divided into low- and high- risk groups based on their risk scores. We found that neither the high-risk patients nor the total study population benefitted from ACT after CCRT. This study can help identify clinical outcomes and provide a basis for further changes in clinical treatment decisions and individualized precision therapy.

Radiomics is widely used in the field of oncology. This research study established an MRI-based radiomics signature for assessing OS in LACSC. Ten radiomics features associated with the OS of LACSC patients were identified in this study, including one GLRLM feature, two GLDM features, two GLCM features, four GLSZM

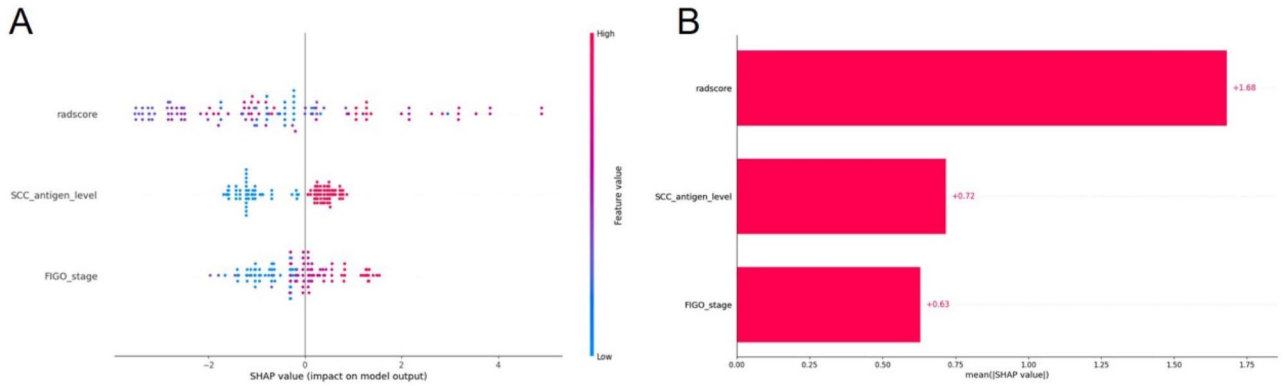

Fig. 6 (**A**) Shapley Additive Explanations (SHAP) summary plot showing the distribution of the SHAP values of each feature. Each dot represents a SHAP value for a feature per patient. The X axis represents the SHAP value, and the color varying from red to blue represents the feature value from high to low, respectively. (**B**) SHAP bar chart showing feature importance according to the mean absolute SHAP value of each feature. SCC, squamous cell carcinoma; FIGO, International Federation of Gynecology and Obstetrics

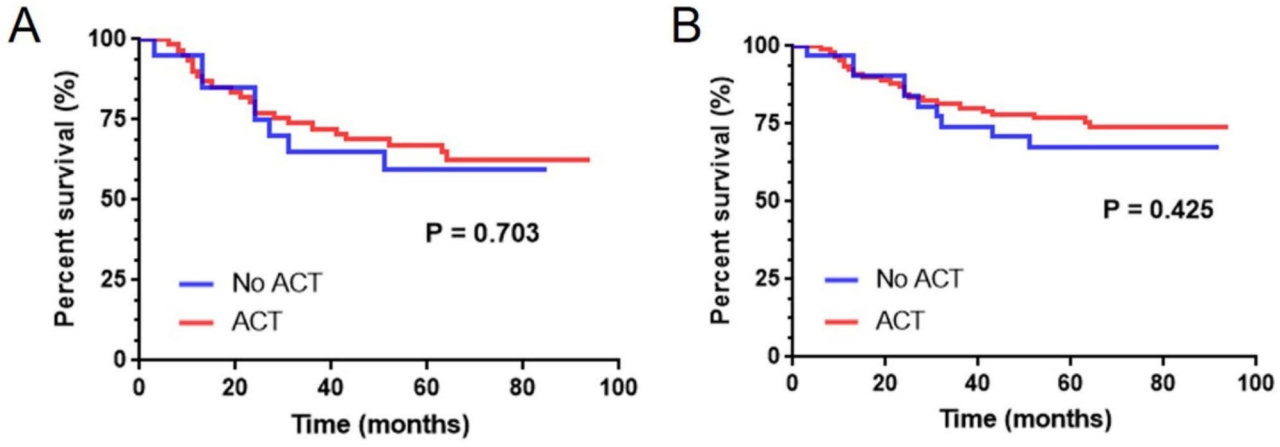

Fig. 7 Kaplan–Meier survival curves of treatment strategy. Stratified according to treatment strategy, for high-risk patients (**A**) and all study patients (**B**). Blue represents patients without ACT after CCRT, and red represents patients with ACT after CCRT. ACT, adjuvant chemotherapy

features, and one shape feature. Radiomics features have been associated with prognosis in multiple diseases because of tumor heterogeneity, including locally advanced rectal cancer [13], hypopharyngeal carcinoma [14], breast cancer [15], and cervical cancer [16]. For example, GLCM and GLRLM could predict the effect of CCRT on LACSC patients [16]. Radiomics features with higher values correlate with worse outcomes, proving a negative relationship between heterogeneous tumors and prognosis [17]. Accumulating evidence suggested that in radiological images, texture analysis may yield additional predictive and prognostic information that related to underlying spatial variation and heterogeneity of voxel intensities within tumors [18]. Wang et al. [19] also found that radiomics may provide valuable information regarding differentiation and composition of tumor cells in the tumor microenvironment, and considered that radiomics helps improve individualized estimations of disease-free survival and guide treatment strategies for patients with breast cancer. At the same time, the application of various machine learning, deep learning and artificial intelligence is also gradually emerging in clinical research. Wing-Keen Yap et al. [20] using machine learning algorithm to integrate radiotherapy dose distribution information, obtained an accurate model for predicting pathological complete response of neoadjuvant chemoradiotherapy for esophageal cancer through 5-fold cross-validation. In addition, a retrospective, multicohort, diagnostic study [21] indicated that the deep convolutional neural network (DCNN) model showed similar sensitivity and improved specificity in identifying patients with thyroid cancer compared with a group of skilled radiologists, with area under the curve values of 0.947 (95% CI 0.935-0.959) for the internal validation set, and 0.912 (95% CI 0.865-0.958), 0.908 (95% CI 0.891-0.925)for two external validation sets respectively. There was also a study [22] using machine learning algorithms to predict the prognosis of patients with stage IV lung cancer, which improves the

accuracy of prognosis prediction and has a high universality of mechanisms. Our research confirmed the notion that radscore was prognostic factor (Fig. 3, $P = 0.010$). In the future, radiomics signature may be used as a noninvasive clinical biomarker for predicting OS in LACSC patients undergoing CCRT.

Two other independent prognostic factors, SCC antigen level and FIGO stage, were identified by univariate and multivariate Cox analyses. In cervical cancer patients, various biomarkers have been identified as prognostic factors, such as FIGO stage, SCC antigen level, tumor volume, and lymph node metastasis [23–26]. In our study, FIGO stage was associated with OS in all patients (overall, $P = 0.002$; training set, $P = 0.009$; and testing set, $P = 0.193$). This may be due to the large variation in the number of cases for each FIGO stage.

We build a nomogram using the radscore and clinical characteristics. The OS of cervical cancer patients can be directly visualized via nomograms. For patients with HER2-positive invasive breast cancer treated using neoadjuvant chemotherapy, Li et al. [15] developed a nomogram based on a combined radiomics and clinicoradiologic model to predict disease-free survival; in the training set, the C-index of this combined model was 0.974, while that of a clinicoradiologic model alone was 0.855. Liu et al. [27] reported that radiomics signature was an independent prognostic factor in locally advanced rectal cancer patients, and that it facilitated individualized treatment planning and the identification of patients who might benefit from ACT for the distant control. Similarly, in our study, the combined model provided more accurate OS predictions for patients with cervical cancer before treatment than the radiomics model and clinical model. It appears that radiomics and clinical factors can be combined to improve prediction performance. At the same time, we used SHAP for further explanation of the combined model, which was rarely used in model analysis. SHAP demonstrated the importance of radiomics, probably because radiomics provides large amount of more accurate tumor information. The clinical advantage of the extraction of MRI-based radiomics features is its noninvasiveness and by utilizing diagnostic images that are already available, so no additional examinations are required. Therefore, this model may be extended to clinical applications. Studies have shown that MRI magnetic intensity and contrast agents have been found to effect radiomics signatures [28, 29]. Thus, it is possible to build more accurate prediction models using 3.0-T enhanced MRI.

It is well-known that the standard treatment of LACSC is CCRT according to the 2022 National Comprehensive Cancer Network guidelines [30]. There is limited evidence that ACT after CCRT is effective and safe for patients with LACSC. A multi-institutional retrospective analysis demonstrated that ACT after CCRT may be a valuable tool in further improving disease control, but due to increased treatment-related complications and severe diarrhea that adversely affected patients' quality of life, post-CCRT ACT was not considered as the best choice in general [31]. A recent OUTBACK study found that older patients (>60-year-old) could benefit more from CCRT alone. Furthermore, ACT after CCRT did not improve 5-year OS and progression-free survival rates in the above study [32]. The present study also produced a similar result, but we considered more influencing factors and targeted at Asian people. As far as we know, this study is the first assessment of a model based on radiomics and clinical factors that can help predict chemotherapy response in cervical cancer patients. We combined independent prognostic factors to obtain a novel risk score. ACT did not improve OS in the high-risk group or in the total study population. For high-risk patients, other strategies may be used to improve OS and decrease the possibility of recurrence, such as targeted therapy and immunotherapy.

Few studies have investigated MRI-based radiomics in LACSC. We established an accurate model to predict the OS of LACSC patients and used SHAP to emphasis the importance of radiomics, and then, used this model to evaluate the value of ACT in this population. Some limitations of our study must be acknowledged. First, relatively few patients with heterogeneous FIGO stages were recruited from a single center. We will recruit more patients and conduct a more detailed stratification study. Second, our research did not contain patients with adenocarcinoma or other histological types of cervical cancer because of their rarity. We intend to accumulate more relevant cases for future research. Finally, this study was not externally validated. We will continue to improve this study in order to provide more basis for precision treatment in the future with the application of radiomics in the clinic.

Conclusion

The present study indicated that the combined model of MRI-based radiomics and clinical characteristics could improve the accuracy of predicting the effects of CCRT in patients with LACSC and radiomics could provide the greatest contribution. This study confirmed that ACT after CCRT did not improve patients' prognosis. In future, the combination of clinical factors and radiomics features may be combined to formulate personalized treatment strategies.

Abbreviations

ACT	Adjuvant chemotherapy
AUC	Area under curve
CCRT	Concurrent chemoradiotherapy
CI	Confidence interval

DFS	Disease free survival
FIGO	International Federation of Gynecology and Obstetrics
GLCM	Gray-level co-occurrence matrix
GLDM	Gray-level dependence matrix
GTV	Gross tumor volume
LACSC	Locally advanced cervical squamous carcinoma
LRC	Loco-regional control
LVSI	Lymphovascular space invasion
MRI	Magnetic resonance imaging
NCCN	National Comprehensive Cancer Network
OS	Overall survival
ROC	Receiver operator characteristic curve
ROI	Region of interest
RQS	Radiomics quality score
SCC	Squamous cell carcinoma
SHAP	Shapley Additive Explanations
SZE	Short-zone emphasis
T2WI	T2-weighted imaging

Acknowledgements
The authors would like to thank all staff in the Department of Gynecological Radiotherapy and Radiology. We also thank Medjaden Inc. for the scientific editing of this manuscript.

Author contributions
All authors contributed to the study conception and design. The study was designed by YW, LNG and YYZ. YFS completed most of the scanning and provided relevant parameters. YYY provided images and performed segmentation. HXZ reviewed the segmentation. YW analyzed the data and wrote the first draft. YZ and JZY provided guidance for manuscript writing. All authors read and approved the final manuscript.

Funding
This study is supported by the National Natural Science Foundation (U20A20339) and Provincial Key R&D Program of Heilongjiang Province (GA21C004).

Data availability
The datasets used and analyzed during the current study available from the corresponding author on reasonable request.

Declarations

Ethics approval and consent to participate
This retrospective study was performed in accordance with the Declaration of Helsinki and was approved by the Ethics Committees of the Harbin Medical University Cancer Hospital (KY2022-22). The requirement for informed consent was waived by the Ethics Committee of Harbin Medical University Cancer Hospital because of the retrospective nature of the study.

Consent for publication
Not applicable.

Competing interests
The authors declare no competing interests.

Author details
[1]Department of Gynecological Radiotherapy, Harbin Medical University Cancer Hospital, 150 Haping Road, Harbin 150081, Heilongjiang Province, China
[2]Department of Radiology, Harbin Medical University Cancer Hospital, Harbin, China

Received: 15 April 2024 / Accepted: 3 February 2025
Published online: 10 February 2025

References

1. Yuan L, Guo J, Zhang X, Chen M, Xu C, Yao L. Feasibility of radical hysterectomy in women with FIGO stage IIB cervical cancer: an observation study of 10-year experience in a tertiary center. Onco Targets Ther. 2018;11:5527–33. https://doi.org/10.2147/OTT.S173208
2. National cancer institute: Cancer stat facts: Cervix uteri cancer. 2021.; Available from: https://seer.cancer.gov/statfacts/html/cervix.html. [Accessed 2022 April 11].
3. Mauricio D, Zeybek B, Tymon-Rosario J, Harold J, Santin AD. Immunotherapy in cervical cancer. Curr Oncol Rep. 2021;23(6):61. https://doi.org/10.1007/s11912-021-01052-8
4. Duenas-Gonzalez A, Zarba JJ, Patel F, Alcedo JC, Beslija S, Casanova L, Orlando M. Phase III, open-label, randomized study comparing concurrent gemcitabine plus cisplatin and radiation followed by adjuvant gemcitabine and cisplatin versus concurrent cisplatin and radiation in patients with stage IIB to IVA carcinoma of the cervix. J Clin Oncol. 2011;29(13):1678–85. https://doi.org/10.1200/JCO.2009.25.9663
5. Yuan Y, You J, Li X, Wang W. Adjuvant chemotherapy after radiotherapy or concurrent chemoradiotherapy for pelvic lymph node-positive patients with locally advanced cervical cancer: a propensity score matching analysis. Int J Gynecol Cancer. 2022;32(1):21–7. https://doi.org/10.1136/ijgc-2020-001230
6. Choi CH, Lee JW, Kim TJ, Kim WY, Nam HR, Kim BG, Bae DS. Phase II study of consolidation chemotherapy after concurrent chemoradiation in cervical cancer: preliminary results. Int J Radiat Oncol Biol Phys. 2007;68(3):817–22. https://doi.org/10.1016/j.ijrobp.2006.12.038
7. Kim HS, Kim MK, Kim HJ, Han SS, Kim JW. Phase II study of consolidation chemotherapy after adjuvant or primary concurrent chemoradiation using paclitaxel and carboplatin to treat high-risk early-stage or locally advanced cervical cancer. Cancer Res Treat. 2012;44(2):97–103. https://doi.org/10.4143/crt.2012.44.2.97
8. Petric Mise B, Jelavic B, Strikic T, Hrepic A, Tomic D, Hamm K, Vrdoljak W, E. Long follow-up of patients with locally advanced cervical cancer treated with concomitant chemobrachyradiotherapy with cisplatin and ifosfamide followed by consolidation chemotherapy. Int J Gynecol Cancer. 2015;25(2):315–9. https://doi.org/10.1097/IGC.0000000000000336
9. Ali N, Valimohammad AT, Abbasi AN, Mansha MA, Hafiz A, Qureshi BM. Chemoradiation and the role of adjuvant chemotherapy in lymph nodal-metastatic cervical cancer. J Glob Oncol. 2018;4:1–4.
10. Liu Z, Wang S, Dong D, Wei J, Fang C, Zhou X, Tian J. The applications of radiomics in precision diagnosis and treatment of oncology: opportunities and challenges. Theranostics. 2019;9(5):1303–22. https://doi.org/10.7150/thno.30309
11. Liu Z, Zhang XY, Shi YJ, Wang L, Zhu HT, Tang Z, Sun YS. Radiomics analysis for evaluation of pathological complete response to neoadjuvant chemoradiotherapy in locally advanced rectal cancer. Clin Cancer Res. 2017;23(23):7253–62. https://doi.org/10.1158/1078-0432.CCR-17-1038
12. Li H, Zhu M, Jian L, Bi F, Zhang X, Fang C, Yu X. Radiomic score as a potential imaging biomarker for predicting survival in patients with cervical cancer. Front Oncol. 2021;11:706043. https://doi.org/10.3389/fonc.2021.706043
13. Meng Y, Zhang Y, Dong D, Li C, Liang X, Zhang C, Zhang H. Novel radiomic signature as a prognostic biomarker for locally advanced rectal cancer. J Magn Reson Imaging. 2018. https://doi.org/10.1002/jmri.25968
14. Mo X, Wu X, Dong D, Guo B, Liang C, Luo X, Zhang S. Prognostic value of the radiomics-based model in progression-free survival of hypopharyngeal cancer treated with chemoradiation. Eur Radiol. 2020;30(2):833–43. https://doi.org/10.1007/s00330-019-06452-w
15. Li Q, Xiao Q, Li J, Duan S, Wang H, Gu Y. MRI-based radiomic signature as a prognostic biomarker for HER2-positive invasive breast cancer treated with NAC. Cancer Manag Res. 2020;12:10603–13. https://doi.org/10.2147/CMAR.S271876
16. Lucia F, Visvikis D, Desseroit MC, Miranda O, Malhaire JP, Robin P, Schick U. Prediction of outcome using pretreatment (18)F-FDG PET/CT and MRI radiomics in locally advanced cervical cancer treated with chemoradiotherapy. Eur J Nucl Med Mol Imaging. 2018;45(5):768–86. https://doi.org/10.1007/s00259-017-3898-7
17. Lucia F, Visvikis D, Vallieres M, Desseroit MC, Miranda O, Robin P, Schick U. External validation of a combined PET and MRI radiomics model for prediction of recurrence in cervical cancer patients treated with chemoradiotherapy. Eur J Nucl Med Mol Imaging. 2019;46(4):864–77. https://doi.org/10.1007/s00259-018-4231-9
18. Chicklore S, Goh V, Siddique M, Roy A, Marsden PK, Cook GJ. Quantifying tumour heterogeneity in 18F-FDG PET/CT imaging by texture analysis. Eur J Nucl Med Mol Imaging. 2013;40(1):133–40. https://doi.org/10.1007/s00259-012-2247-0

19. Wang X, Xie T, Luo J, Zhou Z, Yu X, Guo X. Radiomics predicts the prognosis of patients with locally advanced breast cancer by reflecting the heterogeneity of tumor cells and the tumor microenvironment. Breast Cancer Res. 2022;24(1):20. https://doi.org/10.1186/s13058-022-01516-0
20. Yap W-K, Hsiao I-T, Yap W-L, Tsai T-Y, Lu Y-A, Yang C-K, Cheng S-C. A radiotherapy dose map-guided deep learning method for predicting pathological complete response in esophageal cancer patients after neoadjuvant chemoradiotherapy followed by surgery. Biomedicines. 2023;11(11). https://doi.org/10.3390/biomedicines11113072
21. Li X, Zhang S, Zhang Q, Wei X, Pan Y, Zhao J, Chen K. Diagnosis of thyroid cancer using deep convolutional neural network models applied to sonographic images: a retrospective, multicohort, diagnostic study. Lancet Oncol. 2019;20(2):193–201. https://doi.org/10.1016/s1470-2045(18)30762-9
22. Fujimoto D, Hayashi H, Murotani K et al. Prediction of prognosis in lung cancer using machine learning with inter-institutional generalizability: a multicenter cohort study (WJOG15121L: REAL-WIND). Lung Cancer. 2024; 194 LUNG CANCER. https://doi.org/10.1016/j.lungcan.2024.107896
23. Fu J, Wang W, Wang Y, Liu C, Wang P. The role of squamous cell carcinoma antigen (SCC Ag) in outcome prediction after concurrent chemoradiotherapy and treatment decisions for patients with cervical cancer. Radiat Oncol. 2019;14(1):146. https://doi.org/10.1186/s13014-019-1355-4
24. Klopp AH, Eifel PJ. Biological predictors of cervical cancer response to radiation therapy. Semin Radiat Oncol. 2012;22(2):143–50. https://doi.org/10.1016/j.semradonc.2011.12.009
25. Katanyoo K, Tangjitgamol S, Chongthanakorn M, Tantivatana T, Manusirivithaya S, Rongsriyam K, Cholpaisal A. Treatment outcomes of concurrent weekly carboplatin with radiation therapy in locally advanced cervical cancer patients. Gynecol Oncol. 2011;123(3):571–6. https://doi.org/10.1016/j.ygyno.2011.09.001
26. Rose PG, Java J, Whitney CW, Stehman FB, Lanciano R, Thomas GM, DiSilvestro PA. Nomograms predicting progression-free survival, overall survival, and pelvic recurrence in locally advanced cervical cancer developed from an analysis of identifiable prognostic factors in patients from NRG oncology/gynecologic oncology group randomized trials of chemoradiotherapy. J Clin Oncol. 2015;33(19):2136–42. https://doi.org/10.1200/JCO.2014.57.7122
27. Liu Z, Meng X, Zhang H, Li Z, Liu J, Sun K, Tian J. Predicting distant metastasis and chemotherapy benefit in locally advanced rectal cancer. Nat Commun. 2020;11(1):4308. https://doi.org/10.1038/s41467-020-18162-9
28. Molina D, Perez-Beteta J, Martinez-Gonzalez A, Martino J, Velasquez C, Arana E, Perez-Garcia VM. Lack of robustness of textural measures obtained from 3D brain tumor MRIs impose a need for standardization. PLoS ONE. 2017;12(6):e0178843. https://doi.org/10.1371/journal.pone.0178843
29. Nie K, Shi L, Chen Q, Hu X, Jabbour SK, Yue N, Sun X. Rectal cancer: assessment of neoadjuvant chemoradiation outcome based on radiomics of multiparametric MRI. Clin Cancer Res. 2016;22(21):5256–64. https://doi.org/10.1158/1078-0432.CCR-15-2997
30. NCCN Clinical Practice Guidelines in Oncology-Cervical Cancer. (2022 Version 1)[EB/OL]. http://www.nccn.org
31. Wu N, Su X, Song H, Li Y, Gu F, Sun X, Cheng G. A multi-institutional retrospective analysis of oncologic outcomes for patients with locally advanced cervical cancer undergoing platinum-based adjuvant chemotherapy after concurrent chemoradiotherapy. Cancer Control. 2021;28:1073274821989307. https://doi.org/10.1177/1073274821989307
32. Mileshkin LR, Moore KN, Barnes EH, Gebski V, Narayan K, King MT, Stockler MR. Adjuvant chemotherapy following chemoradiotherapy as primary treatment for locally advanced cervical cancer versus chemoradiotherapy alone (OUTBACK): an international, open-label, randomised, phase 3 trial. Lancet Oncol. 2023;24(5):468–82. https://doi.org/10.1016/s1470-2045(23)00147-x

Publisher's note